Supplement of Atmos. Chem. Phys., 21, 11467–11487, 2021
https://doi.org/10.5194/acp-21-11467-2021-supplement

Atmospheric Chemistry and Physics
Open Access
EGU

Supplement of

Using GECKO-A to derive mechanistic understanding of secondary organic aerosol formation from the ubiquitous but understudied camphene

Isaac Kwadjo Afreh et al.

Correspondence to: Kelley Claire Barsanti (kbarsanti@engr.ucr.edu)

List of Tables

List of Figures

Table S1: SOA data compiled from published chamber studies for photooxidation and ozonolysis of α-pinene and limonene.

Condition	T (K)	$[O_3]_o$ (ppb)	NO_x (ppb)	$[HC]_o$ (ppb)	ΔHC (μg m^{-3})	SOA mass (μg m^{-3})	SOA yield	Reference
α-Pinene photooxidation	312-306		230	150	804.6	44.0	0.06	Kim and Paulson (2013)
α-Pinene photooxidation	310-312-306		110	152	788.8	103.0	0.14	Kim and Paulson (2013)
α-Pinene photooxidation	306-309		50	142	743.9	107.0	0.16	Kim and Paulson (2013)
α-Pinene photooxidation	312-319-315		47	153	683.0	118.0	0.17	Kim and Paulson (2013)
α-Pinene photooxidation	300			51	260.0	46.0	0.18	Mcvay et al. (2016)
α-Pinene photooxidation	300			56	280.0	65.0	0.23	Mcvay et al. (2016)
α-Pinene photooxidation	300			53	240.0	52.0	0.22	Mcvay et al. (2016)
α-Pinene photooxidation	298			51	268.0	72.0	0.27	Mcvay et al. (2016)
α-Pinene photooxidation	297			53	205.0	35.0	0.17	Mcvay et al. (2016)
α-Pinene photooxidation	297			49	195.0	47.0	0.24	Mcvay et al. (2016)
α-Pinene photooxidation	293				616.6	199.0	0.32	Lee et al. (2006b)
α-Pinene photooxidation	298		0		76.8	29.3	0.38	Ng et al. (2007)
α-Pinene photooxidation	298		1		264.2	121.3	0.46	Ng et al. (2007)
α-Pinene photooxidation	296		198		73.4	15.6	0.21	Ng et al. (2007)
α-Pinene photooxidation	299		938		69.8	4.5	0.06	Ng et al. (2007)
α-Pinene photooxidation	298		968		259.2	40.8	0.16	Ng et al. (2007)
α-Pinene photooxidation			0		259.9	63.9	0.25	Chhabra et al. (2011)
α-Pinene photooxidation			400		265.6	53.7	0.20	Chhabra et al. (2011)
Limonene photooxidation	310-305		300	208	1110.4	96-287	0.35	Kim and Paulson (2013)
Limonene photooxidation	309-313		98	140	735.5	34-195	0.35	Kim and Paulson (2013)
Limonene photooxidation	297-299		120	157	801.0	32-214	0.37	Kim and Paulson (2013)
Limonene photooxidation	311-315		41	130	680.0	11-219	0.43	Kim and Paulson (2013)
Limonene photooxidation	308-312-307		39	130	690.6	14-275	0.47	Kim and Paulson (2013)
Limonene photooxidation	313.4		105		109.0	9.5	0.09	Griffin et al. (1999)
Limonene photooxidation	313.4		80.2		186.2	49.6	0.27	Griffin et al. (1999)
Limonene photooxidation	309.4		139		265.2	79.1	0.30	Griffin et al. (1999)
Limonene photooxidation	309.4		140		348.8	120.2	0.34	Griffin et al. (1999)
Limonene photooxidation	294				676.5	394.0	0.58	Lee et al. (2006b)
α-Pinene ozonolysis	299-300	500		143	592.2	28-230	0.46	Kim and Paulson (2013)
α-Pinene ozonolysis	296-299	500		150	724.3	39-271	0.44	Kim and Paulson (2013)
α-Pinene ozonolysis	296-301	500		170	866.2	37-271	0.40	Kim and Paulson (2013)
α-Pinene ozonolysis	296-295	500		160	897.5	71-349	0.45	Kim and Paulson (2013)
α-Pinene ozonolysis	291-293	500		126	669.8	34-215	0.39	Kim and Paulson (2013)
α-Pinene ozonolysis		200		49.5	282.0	42.3	0.15	Kourtchev et al. (2014)
α-Pinene ozonolysis		200		50.5	312.5	50.0	0.16	Kourtchev et al. (2014)

α-Pinene ozonolysis		200		55.2	349.4	55.9	0.16	Kourtchev et al. (2014)
α-Pinene ozonolysis	298	100		290.2 ±23.2	278.1	62.0 ±1.2	0.23	Nah et al. (2016)
α-Pinene ozonolysis	298	100		280.5 ±22.4	267.0	63.0 ±0.8	0.23	Nah et al. (2016)
α-Pinene ozonolysis	298	100		238.7 ±19.1	222.5	50.6 ±1.6	0.23	Nah et al. (2016)
α-Pinene ozonolysis	298	500		274 ±21.9	278.1	87.3 ±0.3	0.32	Nah et al. (2016)
α-Pinene ozonolysis	298	500		264 ±21.2	261.4	75.7 ±0.6	0.29	Nah et al. (2016)
α-Pinene ozonolysis	298	500		236.1 ±18.9	239.2	66.3 ±1.9	0.28	Nah et al. (2016)
α-Pinene ozonolysis	309.9				89.3	7.4	0.08	Griffin et al. (1999)
α-Pinene ozonolysis	309.9				97.3	8.5	0.09	Griffin et al. (1999)
α-Pinene ozonolysis	303.3				169.4	30.3	0.18	Griffin et al. (1999)
α-Pinene ozonolysis	303.3				248.7	46.0	0.18	Griffin et al. (1999)
α-Pinene ozonolysis	308				306.7	52.3	0.17	Griffin et al. (1999)
α-Pinene ozonolysis	308				349.8	65.1	0.19	Griffin et al. (1999)
α-Pinene ozonolysis	308	237		59.2	306.7	54.2	0.18	Yu et al. (1999)
α-Pinene ozonolysis	308	269		67.2	350.3	65.1	0.19	Yu et al. (1999)
α-Pinene ozonolysis	306	74		107.1	244.3	38.8	0.16	Yu et al. (1999)
α-Pinene ozonolysis	293				1052.2	417.0	0.41	Lee et al. (2006a)
α-Pinene ozonolysis	298.15±12	300			126.8	35.6	0.28	Chen et al. (2011)
α-Pinene ozonolysis	298.15±13	300			11.7	1.2	0.10	Chen et al. (2011)
α-Pinene ozonolysis	298.15±14	300			15.6	1.9	0.12	Chen et al. (2011)
α-Pinene ozonolysis	298.15±15	300			78.9	15.4	0.20	Chen et al. (2011)
α-Pinene ozonolysis	298.15±16	300			506.5	95.2	0.19	Chen et al. (2011)
α-Pinene ozonolysis	298.15±17	300			506.5	138.0	0.27	Chen et al. (2011)
α-Pinene ozonolysis	298.15±18	300			36.7	7.0	0.19	Chen et al. (2011)
α-Pinene ozonolysis	298.15±19	300			5.0	0.5	0.10	Chen et al. (2011)
α-Pinene ozonolysis			0		278.1	62.0	0.22	Chhabra et al. (2011)
Limonene ozonolysis	298-300	500		167	925.8	579.0	0.78	Kim and Paulson (2013)
Limonene ozonolysis	293-295	500		198	1116.3	614.0	0.72	Kim and Paulson (2013)
Limonene ozonolysis	294-296	500		150	842.8	454.0	0.72	Kim and Paulson (2013)
Limonene ozonolysis	295-296	69.7	33.7	154	257.0	135.7	0.49	Chen et al. (2017)
Limonene ozonolysis	295-296	71	35.2	150	269.0	137.2	0.51	Chen et al. (2017)
Limonene ozonolysis	295-297	72.1	58.9	158	220.0	156.5	0.73	Chen et al. (2017)
Limonene ozonolysis	296-297	70.3	62.4	153	228.0	157.3	0.72	Chen et al. (2017)
Limonene ozonolysis	296-297	1.1	67.1	155	144.0	30.3	0.27	Chen et al. (2017)
Limonene ozonolysis	295-296	0.9	68.2	159	138.0	31.8	0.30	Chen et al. (2017)

Table S2: Normalized emission factor (EF) for model surrogates representing top five monoterpenes (by EF) from black spruce, Douglas fir, and lodgepole pine (Hatch et al., 2015, 2017). In Assignment 1, α-pinene is used to represent all monoterpenes except limonene. In Assignment 2, camphene is represented as 50 % α-pinene and 50 % limonene. EFs of assignments 1 and 2 for lodgepole pine are the same, because camphene is not one of the top five monoterpenes by EF.

	Black Spruce		**Douglas Fir**		**Lodgepole Pine**	
	$EF_{\alpha pin}$	EF_{lim}	$EF_{\alpha pin}$	EF_{lim}	$EF_{\alpha pin}$	EF_{lim}
Assignment 1	0.81	0.19	0.8	0.2	0.86	0.14
Assignment 2	0.62	0.38	0.6	0.4	0.86	0.14

Table S3: Two-product SOA yield parameters for α-pinene and limonene based on Griffin et al. (1999).

	2-product			
	α_1	α_2	C^*_1	C^*_2
α-pinene	0.038	0.326	5.8	250.0
limonene	0.239	0.363	18.2	188.7

Table S4: Volatility basis set (VBS) parameters (low NO_x, dry) based on Pathak et al. (2007b) (for α-pinene) and Zhang et al. (2006) (for limonene).

	VBS (low NO_x)				
C*	0	1	10	100	1000
α-pinene	-	0.07	0.038	0.179	0.3
limonene	0.03	0.29	0.31	0.3	0.6

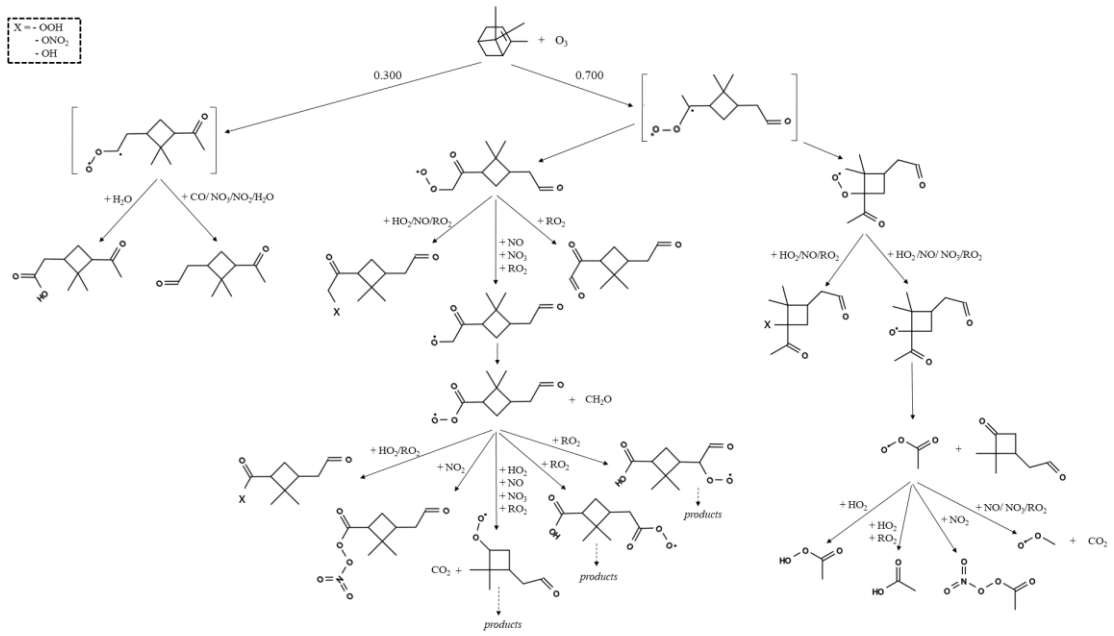

Figure S1: Initial oxidation pathways of α-pinene with O_3 as represented in GECKO-A (inorganic products are not shown).

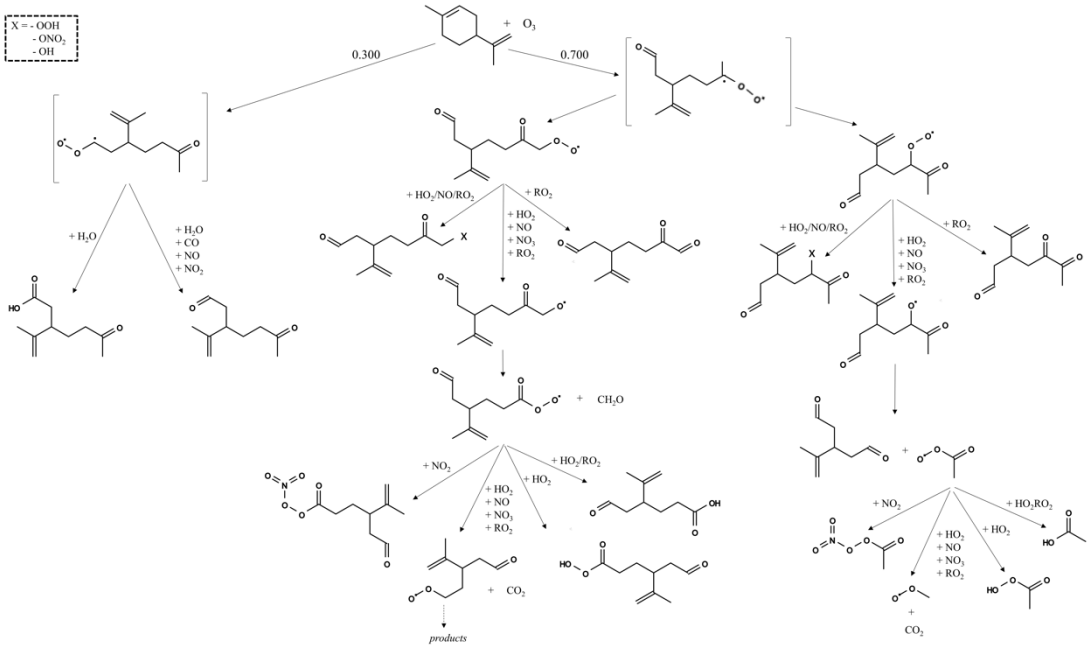

Figure S2: Initial oxidation pathways of limonene with O_3 as represented in GECKO-A (inorganic products are not shown).

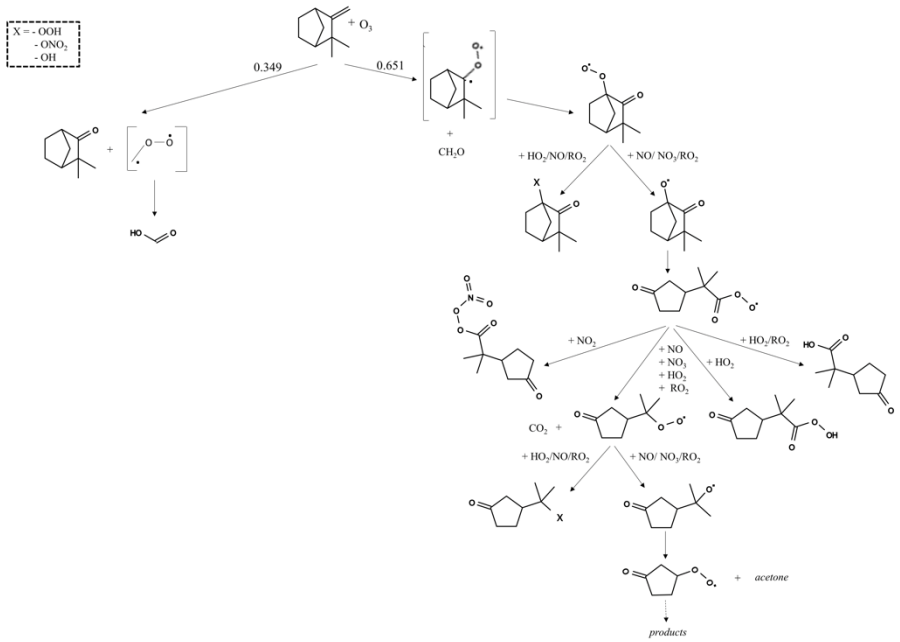

Figure S3: Initial oxidation pathways of camphene with O_3 as represented in GECKO-A (inorganic products are not shown).

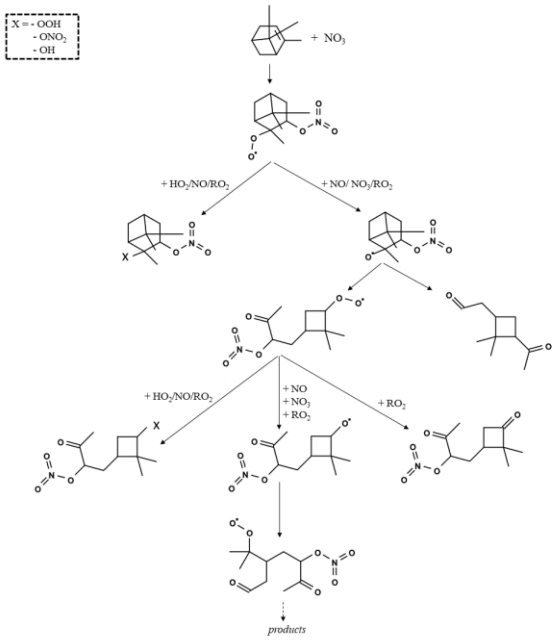

Figure S4: Initial oxidation pathways of α-pinene with NO_3 as represented in GECKO-A (inorganic products are not shown).

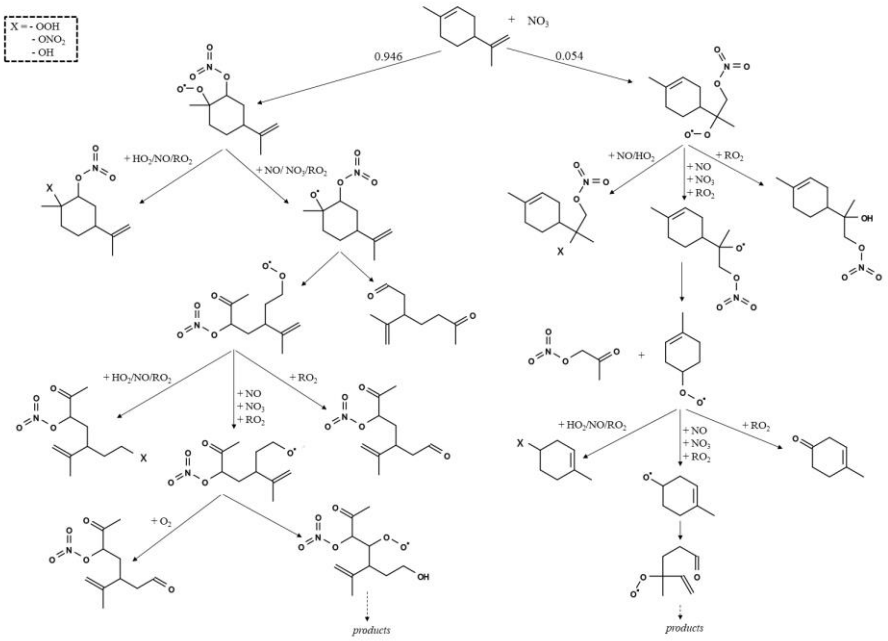

Figure S5: Initial oxidation pathways of limonene with NO_3 as represented in GECKO-A (inorganic products are not shown).

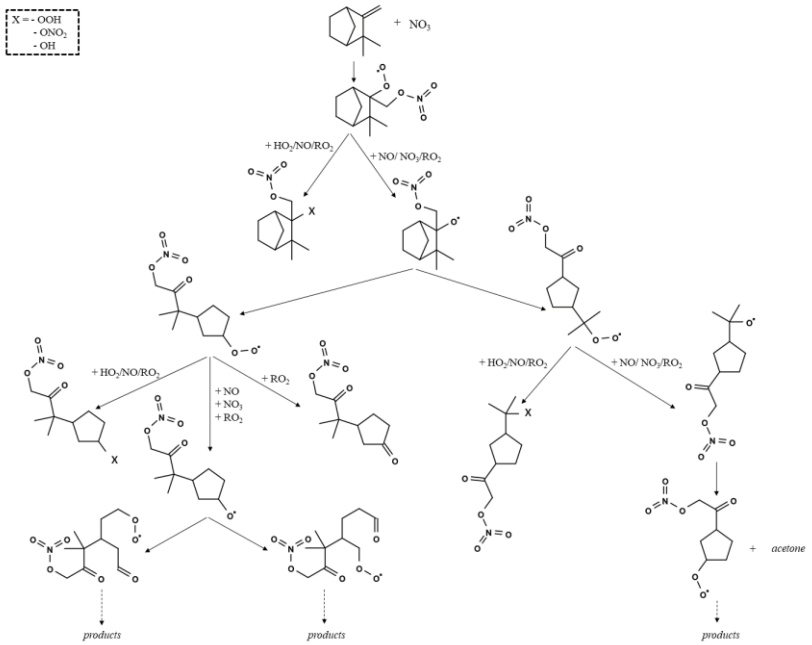

Figure S6: Initial oxidation pathways of camphene with NO_3 as represented in GECKO-A (inorganic products are not shown).

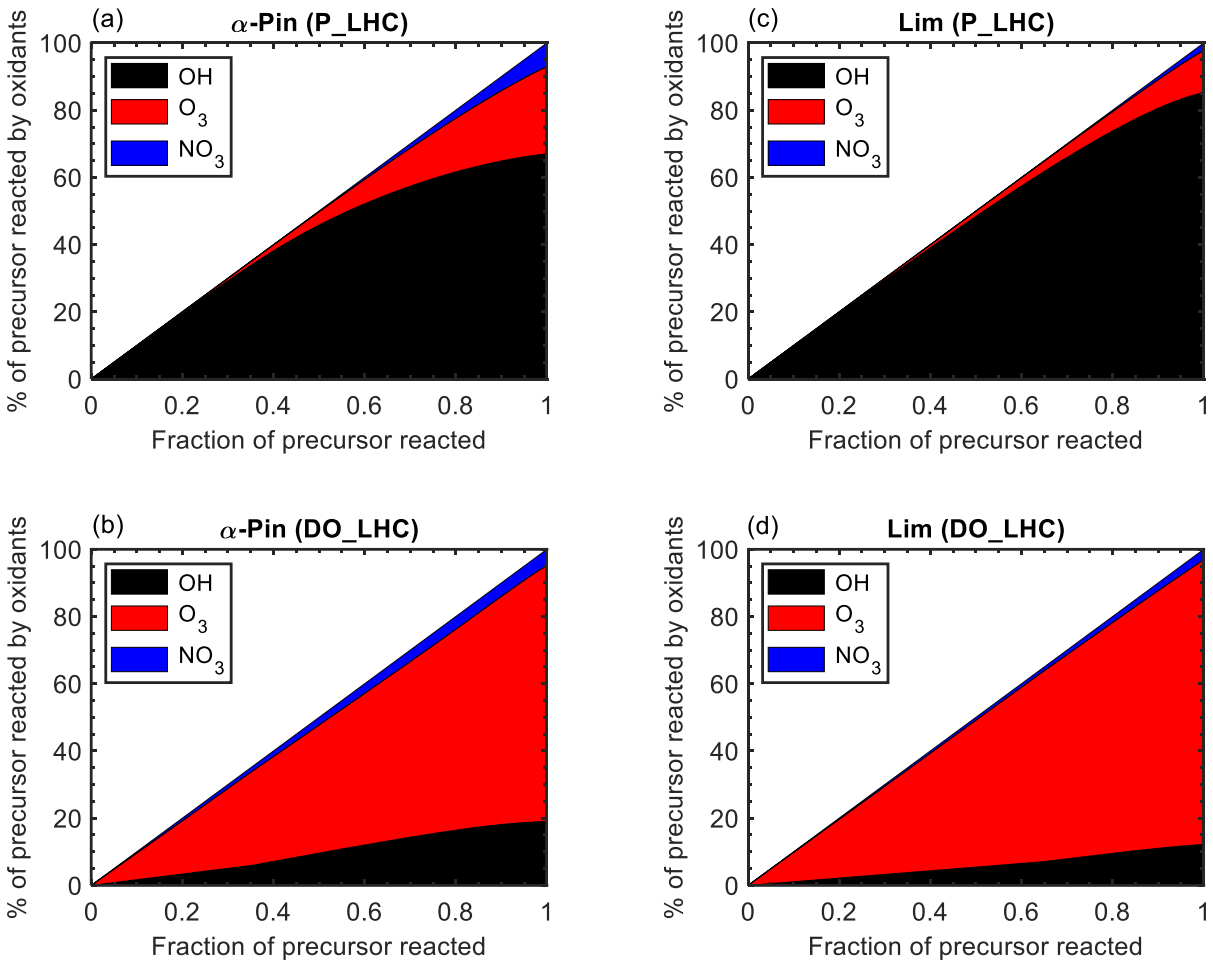

Figure S7: Percentage of precursor consumed by OH (black), O_3 (red), and NO_3 (blue) as a function of fraction of precursor reacted for α-pinene and limonene under photooxidation and ozonolysis (for lower initial precursor mixing ratio of 50 ppb).

Figure S7 shows the percentage of the simulated precursor consumed by the three main oxidants: hydroxyl radical (OH), ozone (O_3), and nitrate radical (NO_3). Under photooxidation, both α-pinene and limonene initially react predominantly with OH. As the reaction progresses (after ~ 30 % of the precursor is reacted), removal of the precursor by O_3 and NO_3 begins to grow until the precursor is completely reacted. The results in Fig. S7a indicate that ~67 % of α-pinene is removed by OH, 25 % by O_3, and ~8 % by NO_3; similarly, as shown in Fig. S7c 85% of limonene is removed by OH, 12% by O_3 and 3 % by NO_3 during photooxidation. For α-pinene ozonolysis, the consumption is largely by O_3 (~75 %) and OH (~20 %), to a lesser extent by NO_3 (~5 %); for limonene, consumption is dominated by O_3 (~85 %), followed by OH (~10 %), and NO_3 (~5 %). Unlike in many chamber experiments, there is no OH scrubber in the simulations. Also, as NO_3 is formed by reaction of O_3 with NO_2 during the dark ozonolysis simulation, a small percentage of the precursor reacts with NO_3 since no light is available to photolyze the NO_3.

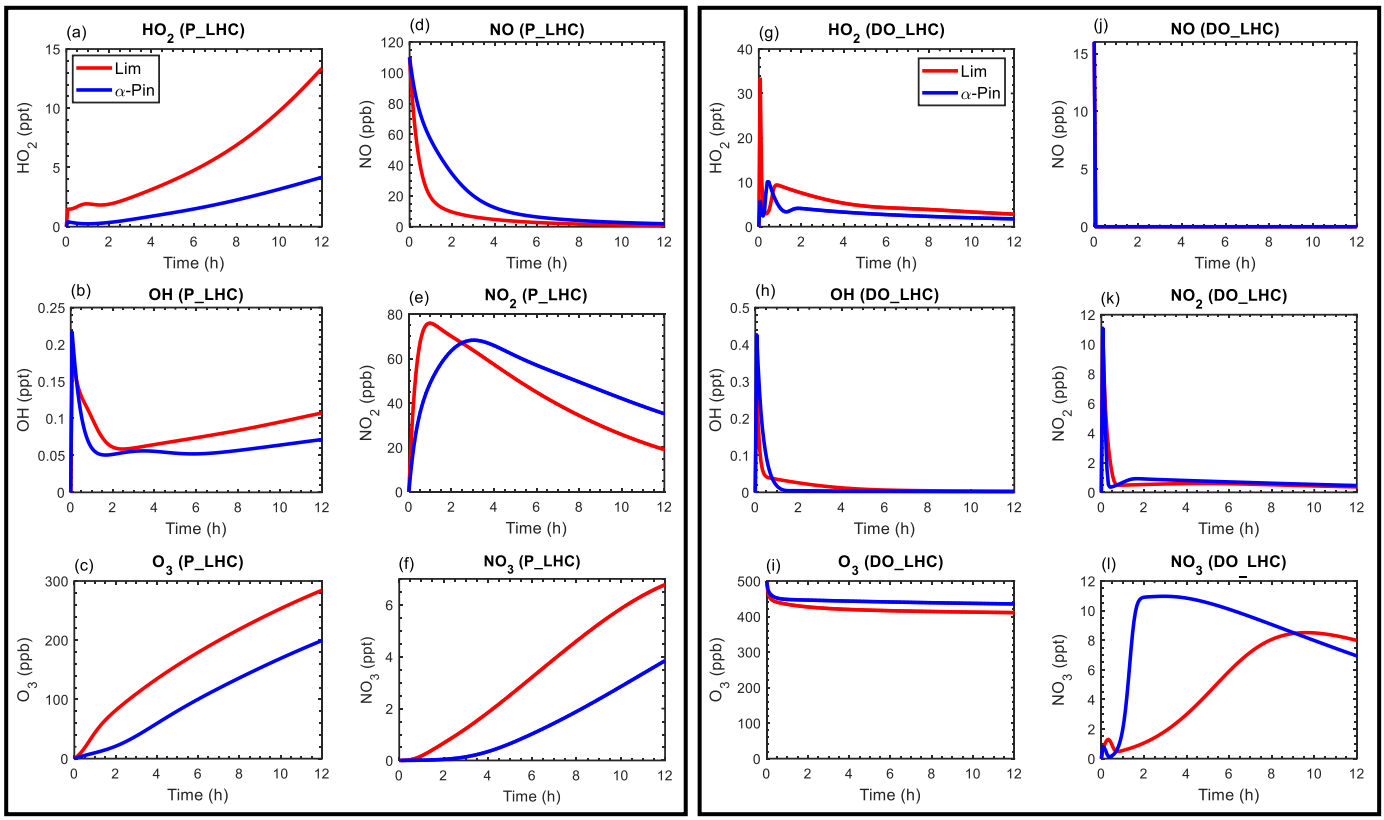

Figure S8: The mixing ratios of HO_2, OH, O_3, NO, NO_2, and NO_3 as a function of time for α-pinene (blue line) and limonene (red line) (with the low initial hydrocarbon (LHC) mixing ratio of 50 ppb) during photooxidation (P) and dark ozonolysis (DO) simulations.

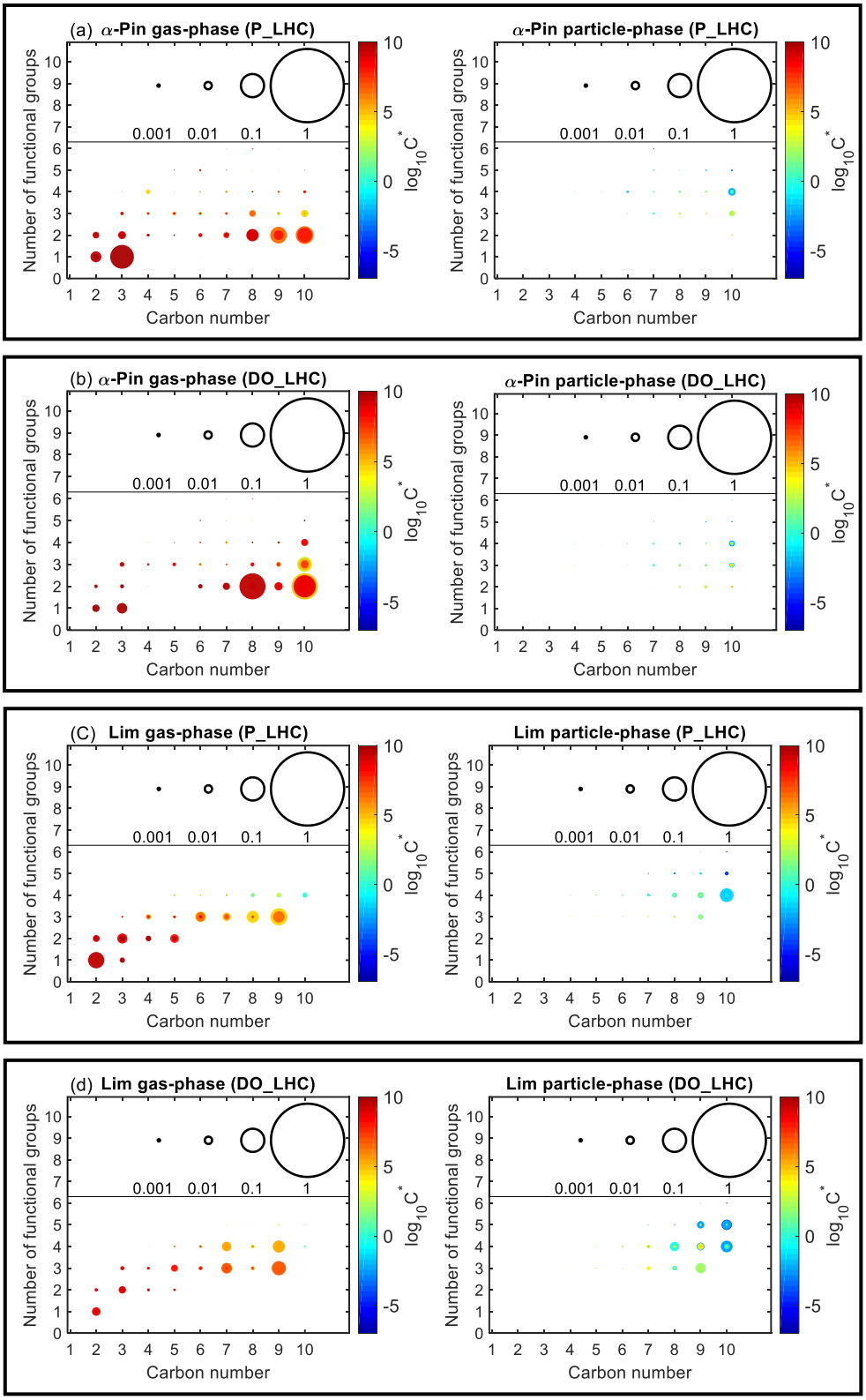

Figure S9: Number of functional groups associated with gas- and particle-phase species as a function of carbon number. Results are shown for camphene, α-pinene, and limonene after 12 hours of oxidation under photooxidation (P) and dark ozonolysis (DO) with lower hydrocarbon (LHC) mixing ratio of 50 ppb. The markers are sized by the ratio of their mixing ratio (in ppbC) to the initial mixing ratio of the precursor (in ppbC). The colors of the markers are scaled by volatility (represented by saturation concentration, C*).

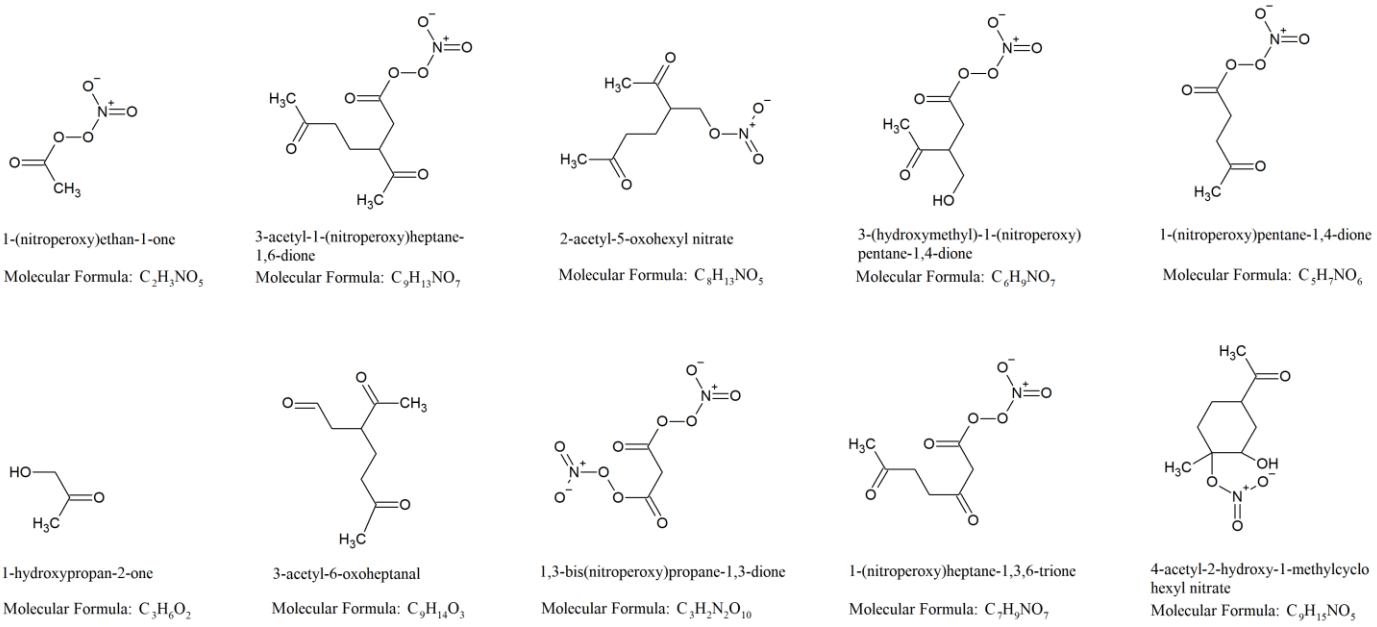

Figure S10: Top 10 gas-phase products from limonene photooxidation at the end of the low hydrocarbon (P_LHC) simulation.

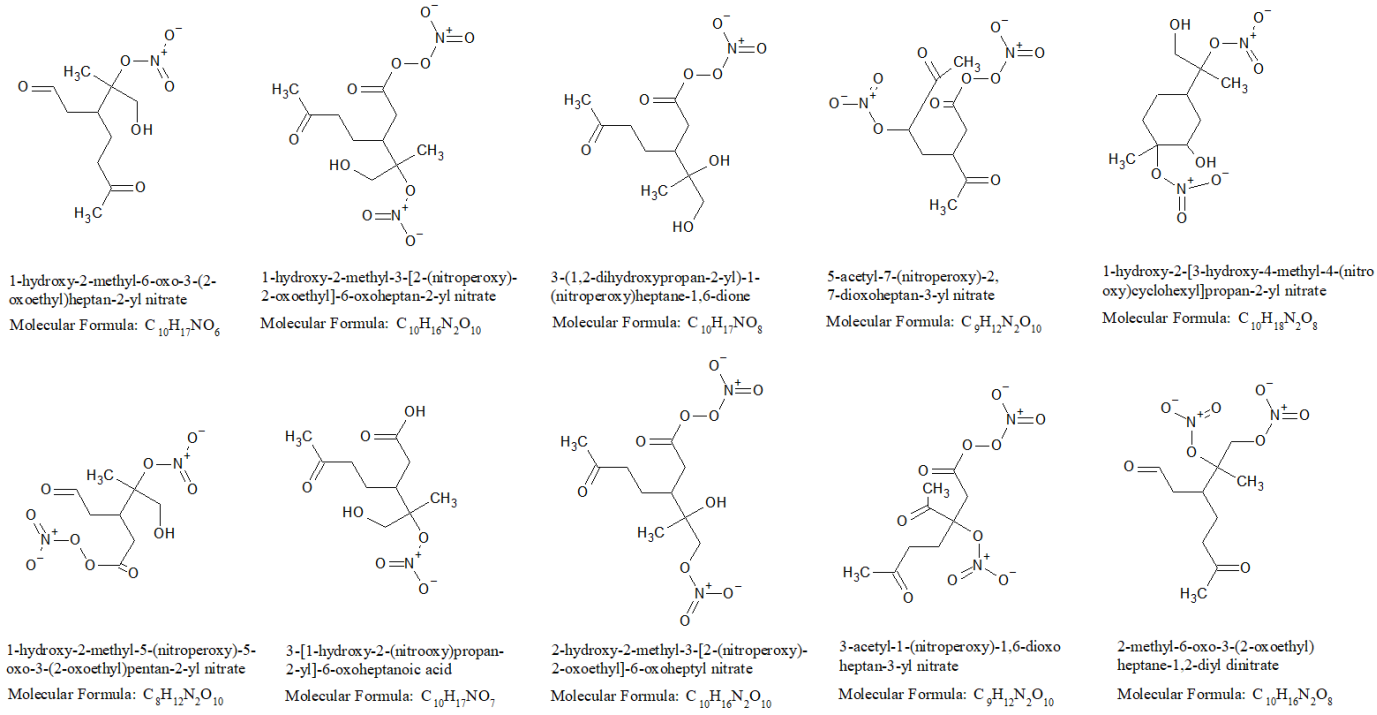

Figure S11: Top 10 particle-phase products from limonene photooxidation at the end of the low hydrocarbon (P_LHC) simulation.

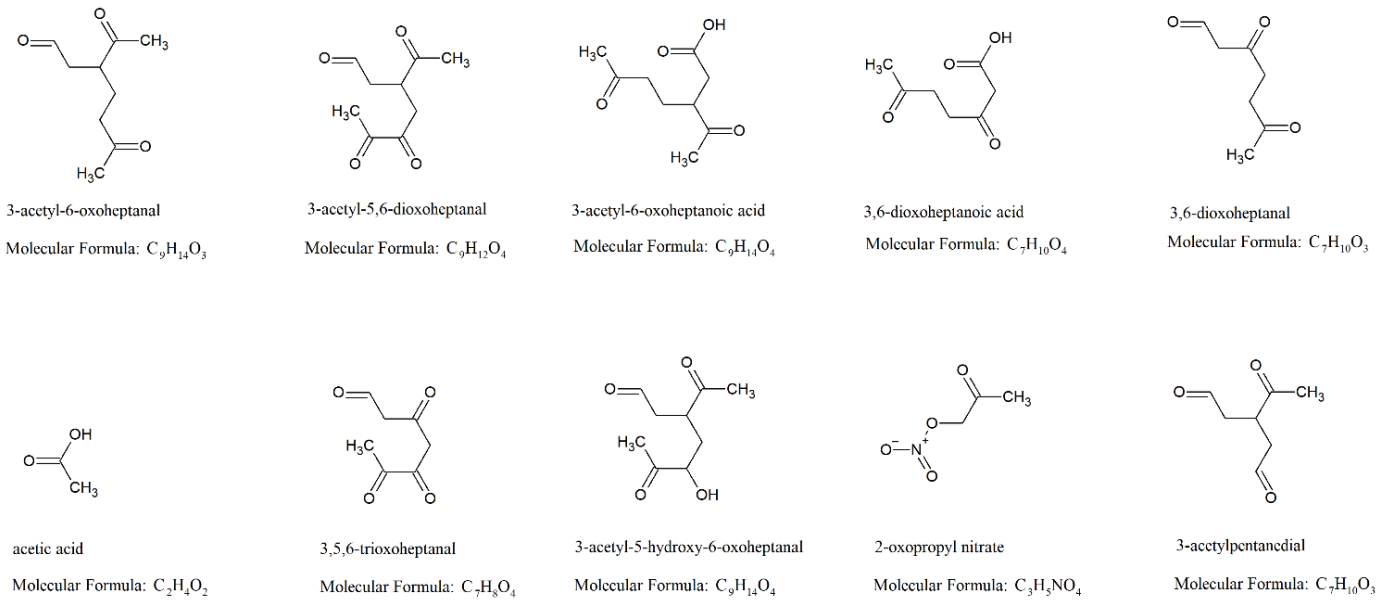

Figure S12: Top 10 gas-phase products from limonene dark ozonolysis at the end of the low hydrocarbon (DO_LHC) simulation.

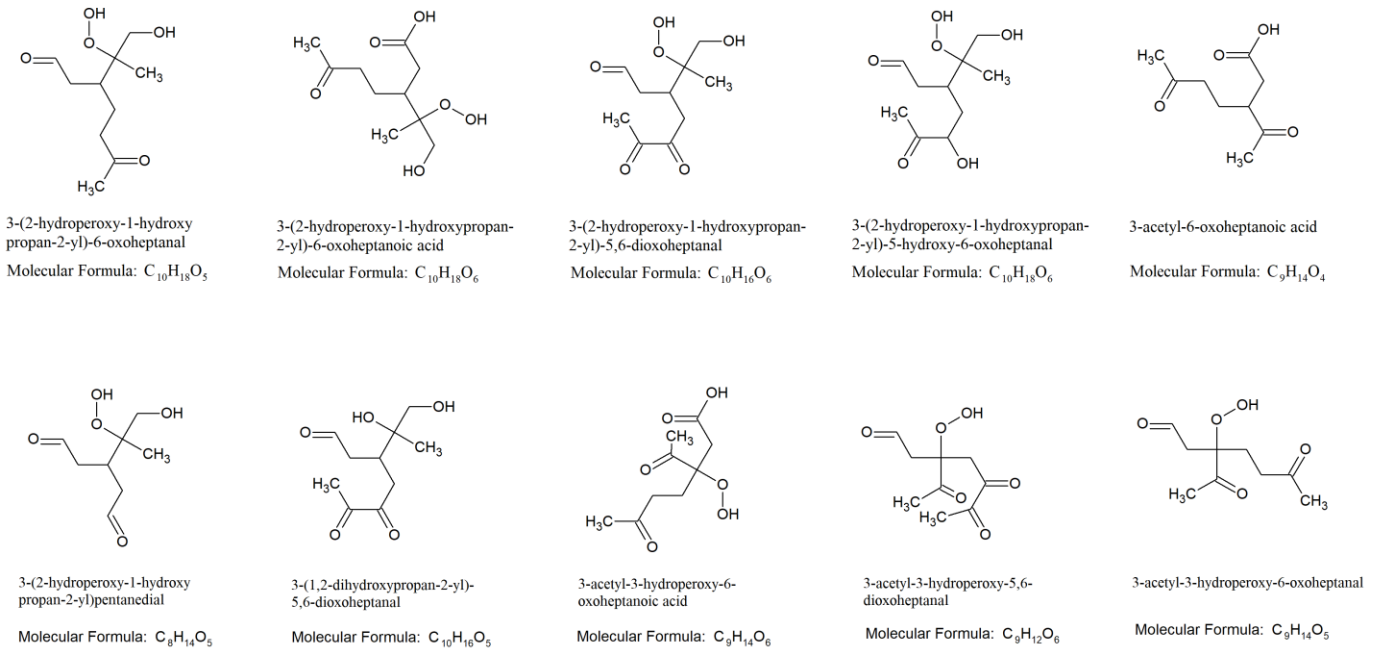

Figure S13: Top 10 particle-phase products from limonene dark ozonolysis at the end of the low hydrocarbon (DO_LHC) simulation.

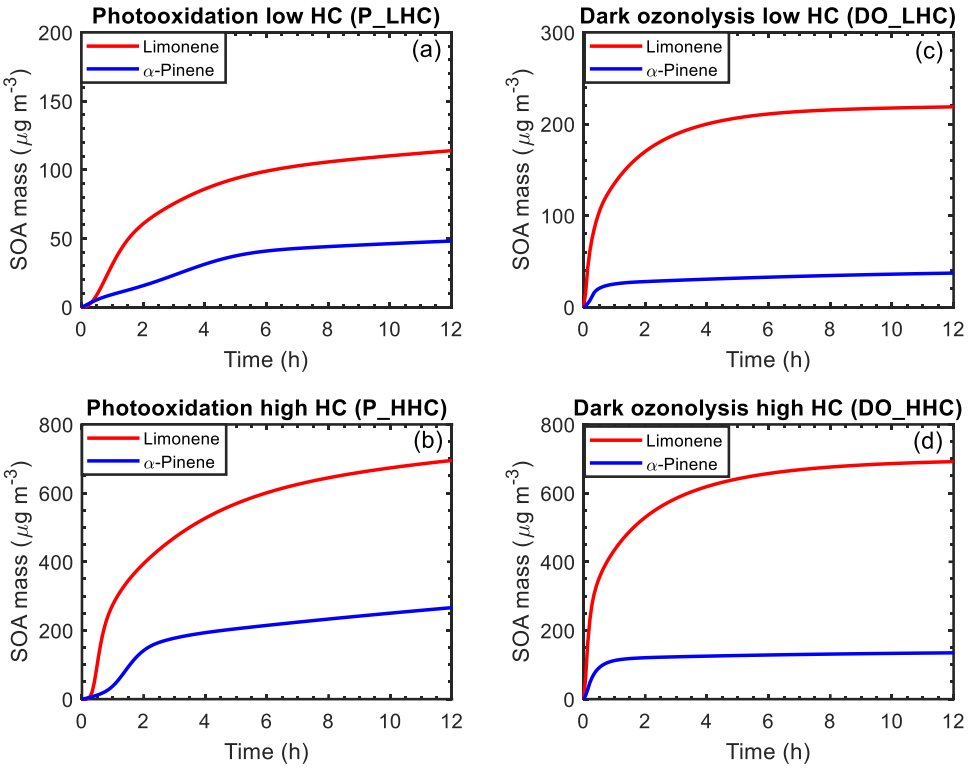

Figure S14: Simulated SOA mass as a function of time for α-pinene and limonene during photooxidation and dark ozonolysis with low hydrocarbon mixing ratio (50 ppb).

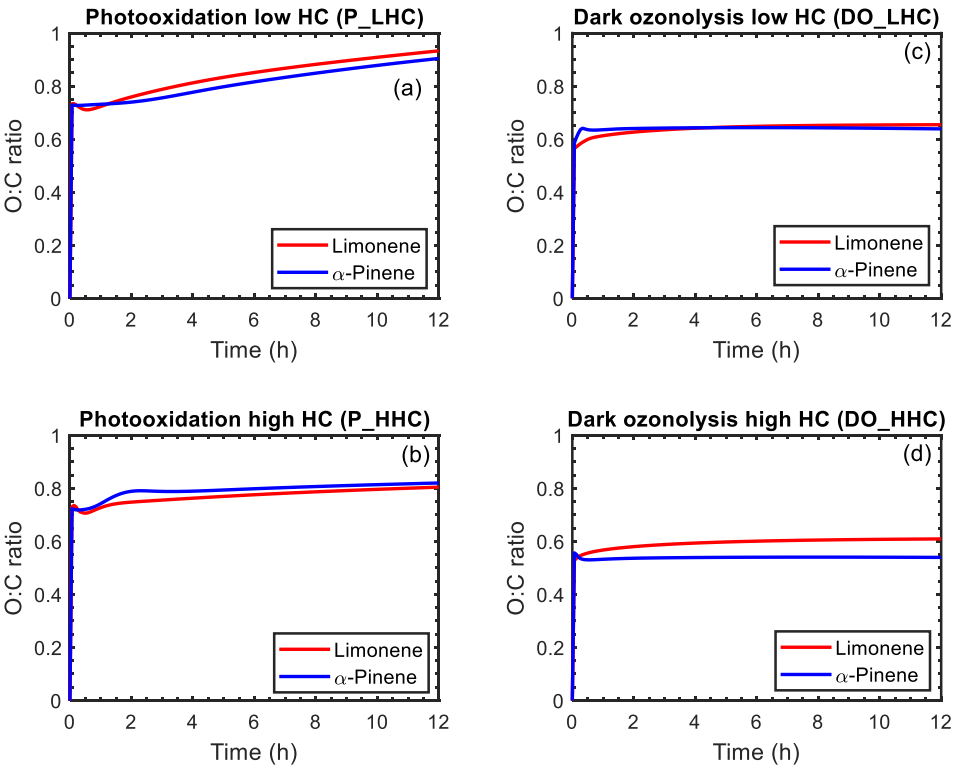

Figure S15: Simulated average O/C as a function of time for α-pinene and limonene during photooxidation and dark ozonolysis with low hydrocarbon mixing ratio (50 ppb).

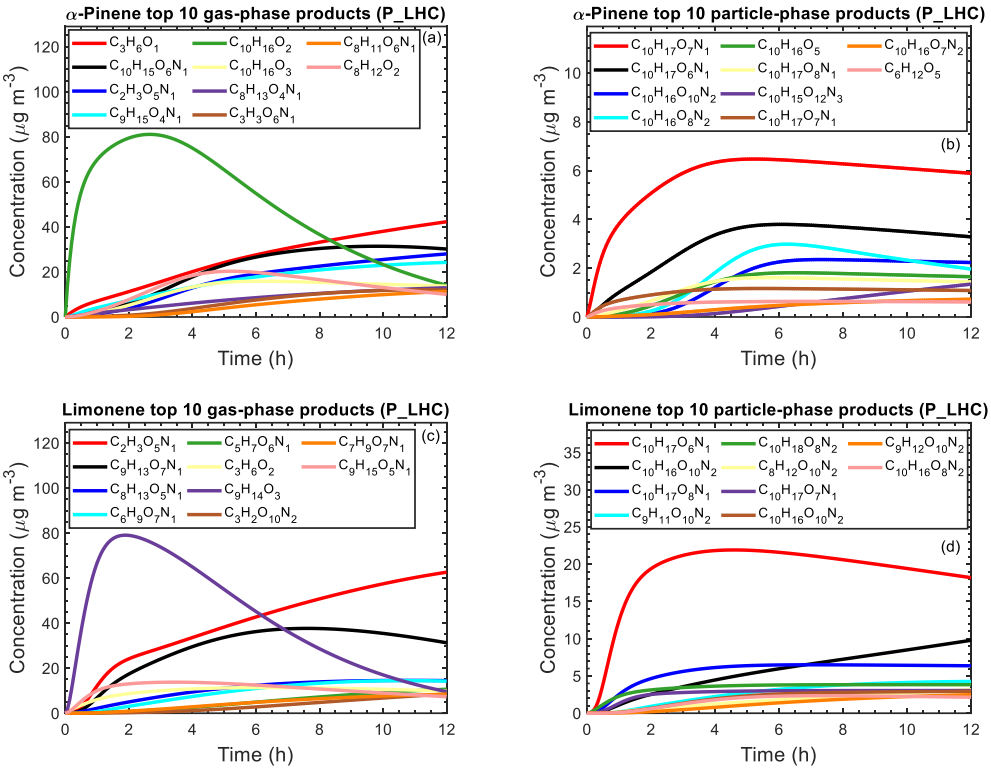

Figure S16: Concentration of top 10 gas- and particle-phase products as a function of time for α-pinene and limonene during photooxidation with low hydrocarbon mixing ratio (50 ppb).

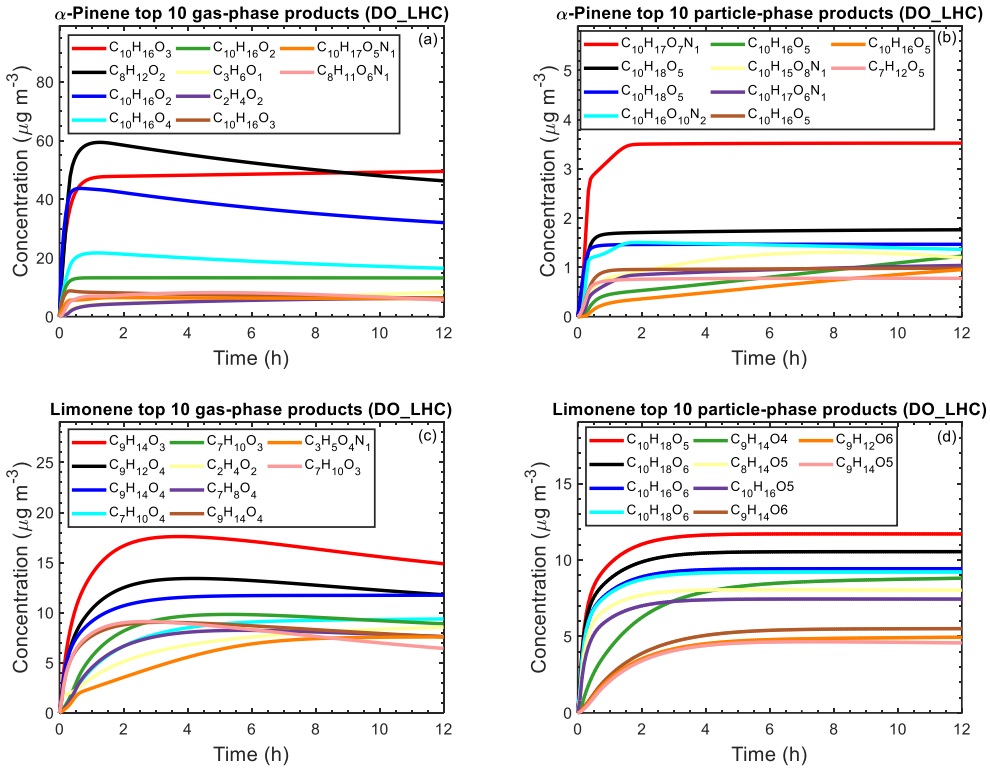

Figure S17: Concentration of top 10 gas- and particle-phase products as a function of time for α-pinene and limonene during dark ozonolysis with low hydrocarbon mixing ratio (50 ppb).

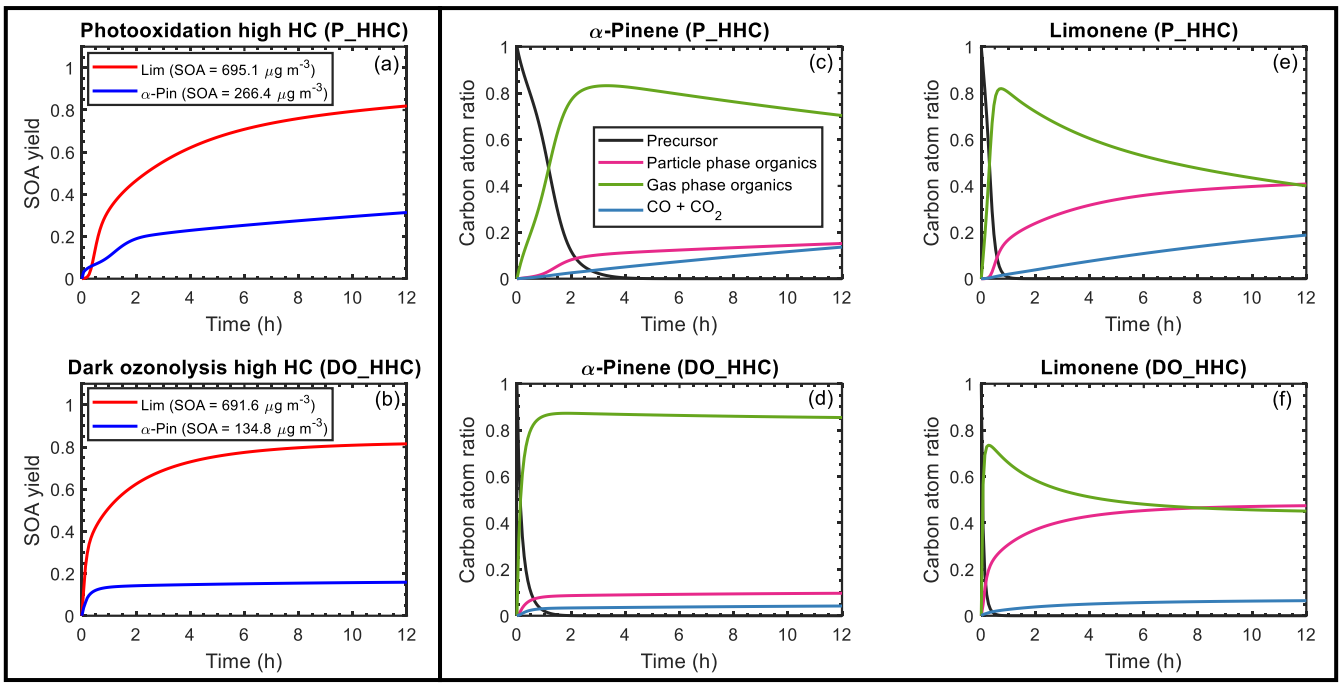

Figure S18: Simulated SOA yield as a function of time (a and b) and carbon budget (c to f) for α-pinene and limonene during photooxidation (a, c, e) and dark ozonolysis (b, d, f). The SOA yield curve for α-pinene is represented by a blue line; limonene is represented by a red line. For the carbon budget plots, the mixing ratios of the precursor (black line), particle-phase organics (magenta line), gas-phase organics (green line), and $CO+CO_2$ (blue line) are expressed as carbon atom ratios (in ppbC)/initial precursor (in ppbC). The results shown are for the high hydrocarbon mixing ratio (150 ppb) simulations.

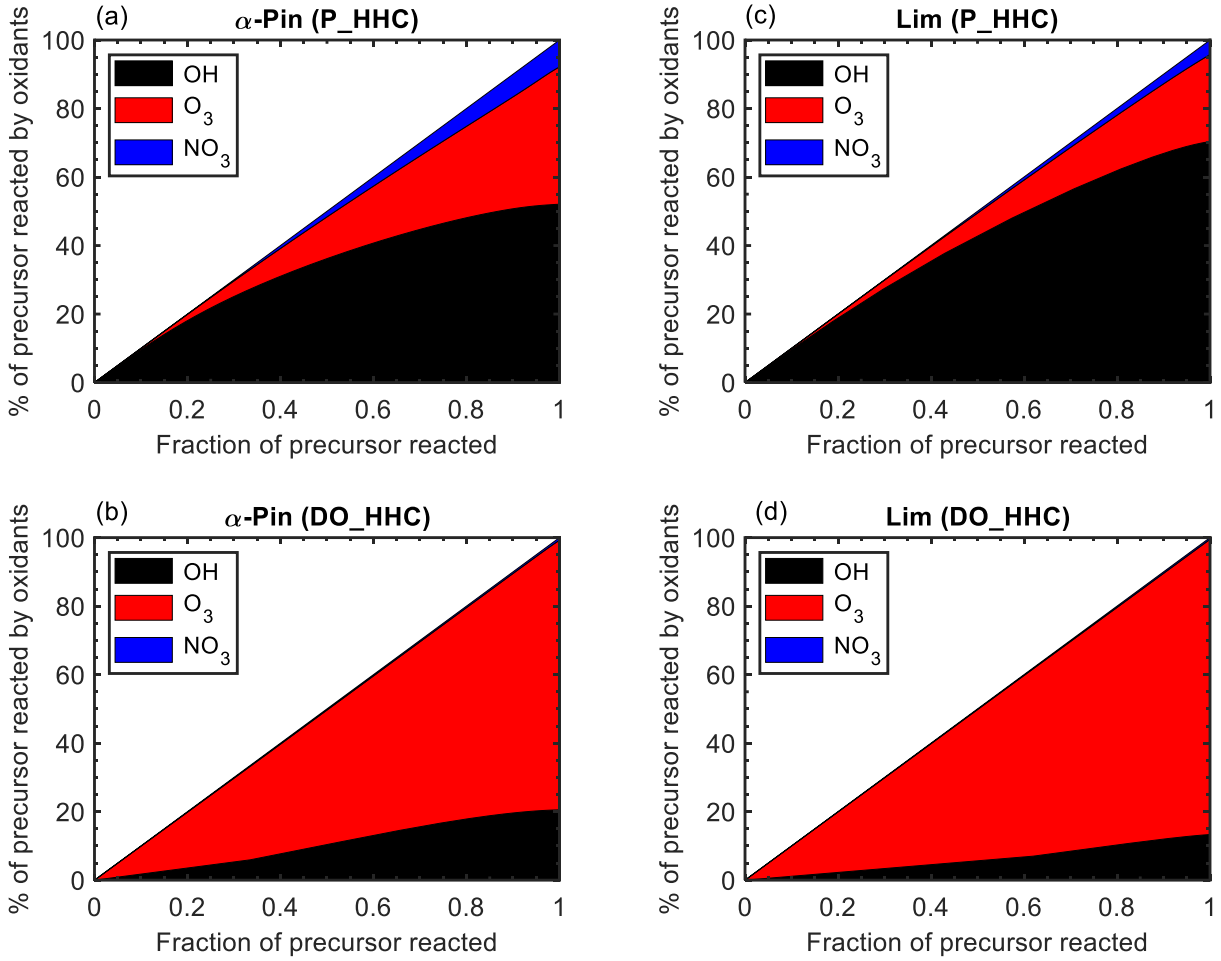

Figure S19: Percentage of precursor consumed by OH (black), O_3 (red), and NO_3 (blue) as a function of fraction of precursor reacted for α-pinene and limonene under photooxidation and ozonolysis (for higher initial precursor concentration of 150 ppb).

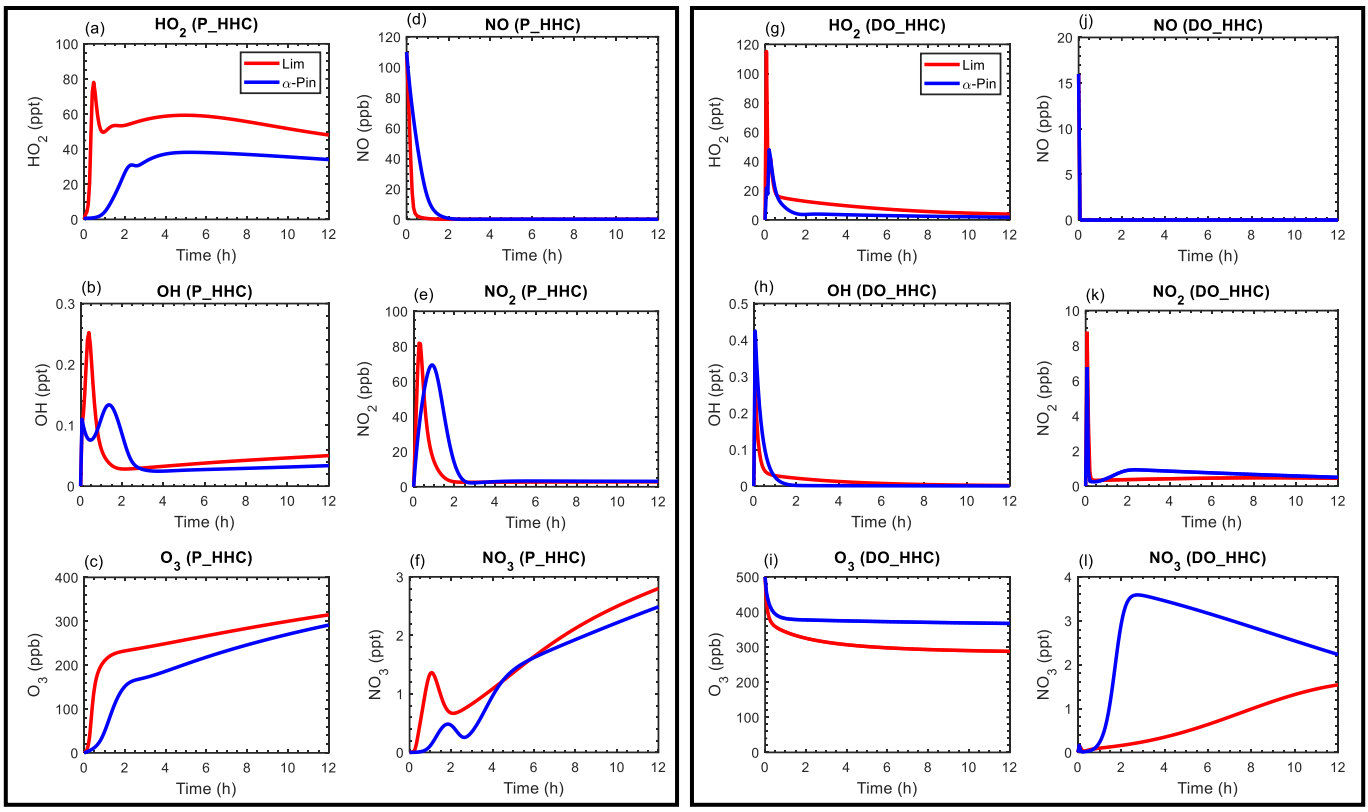

Figure S20: Mixing ratios of HO_2, OH, O_3, NO, NO_2, and NO_3 as function of time for limonene (red line), camphene (black line), and α-pinene (blue line) during the photooxidation and ozonolysis (with higher initial hydrocarbon mixing ratio of 150 ppb).

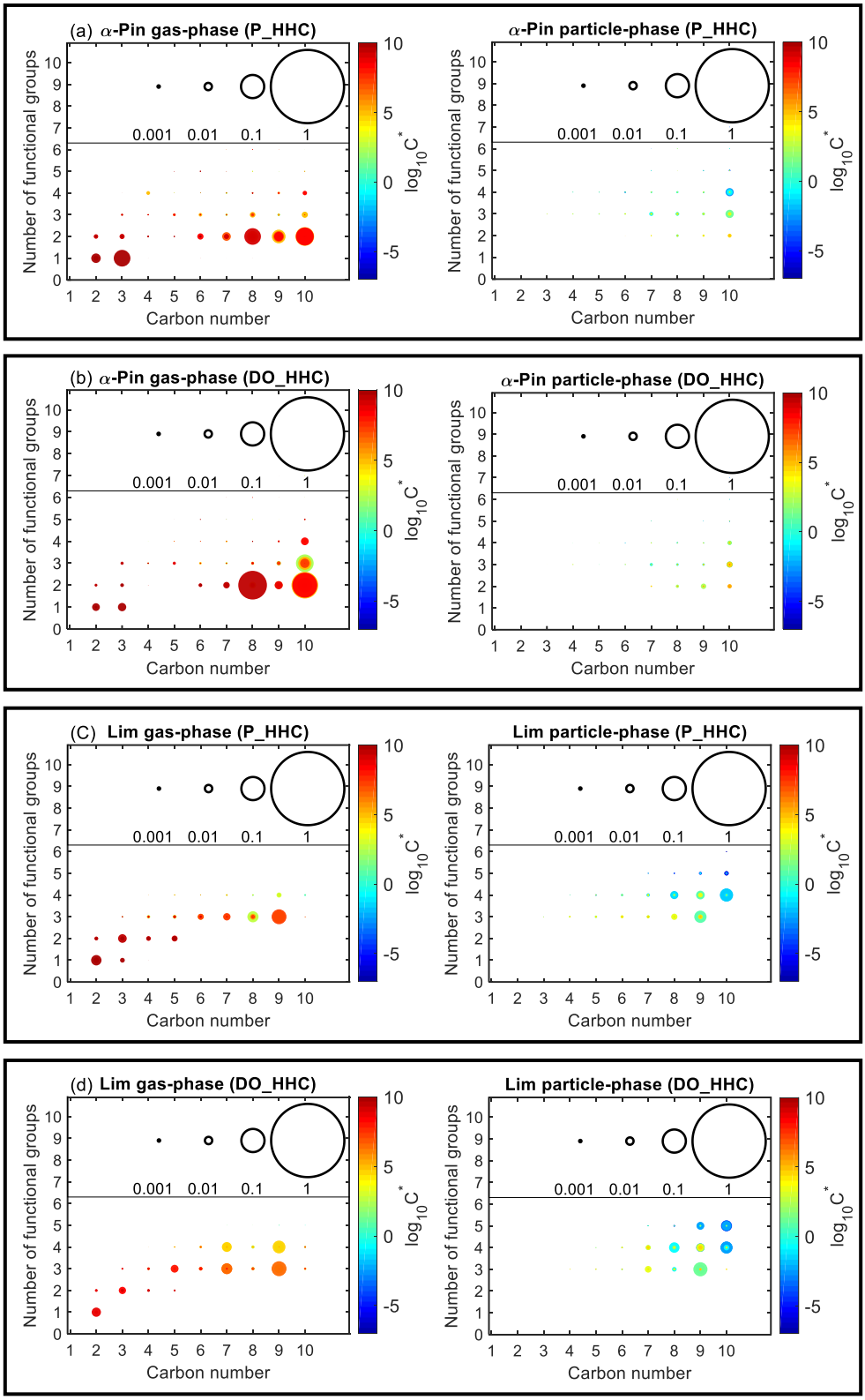

Figure S21: Number of functional groups associated with gas- and particle-phase species as a function of carbon number. Results are shown for camphene, α-pinene, and limonene after 12 hours of oxidation under photooxidation (P) and dark ozonolysis (DO) with higher hydrocarbon (LHC) mixing ratio of 150 ppb. The markers are sized by the ratio of their mixing ratio (in ppbC) to the initial mixing ratio of the precursor (in ppbC). The colors of the markers are scaled by volatility (represented by saturation concentration, C*).

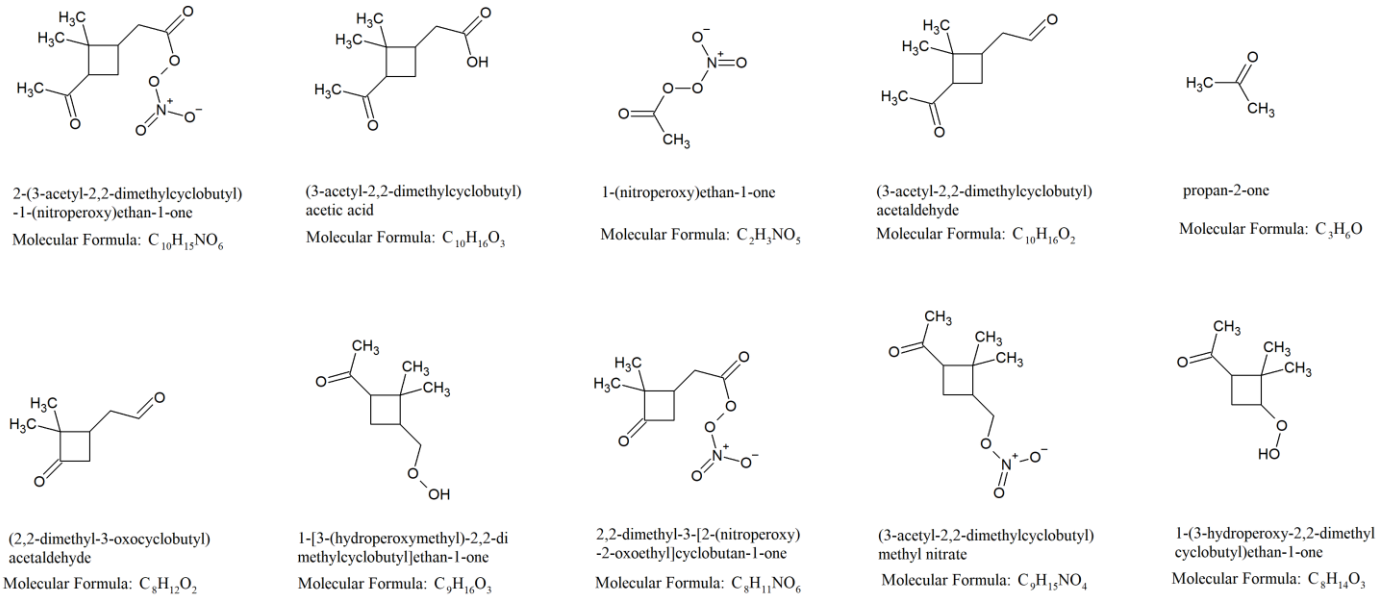

Figure S22: Top 10 gas-phase products from α-pinene photooxidation at the end of the high hydrocarbon (P_HHC) simulations.

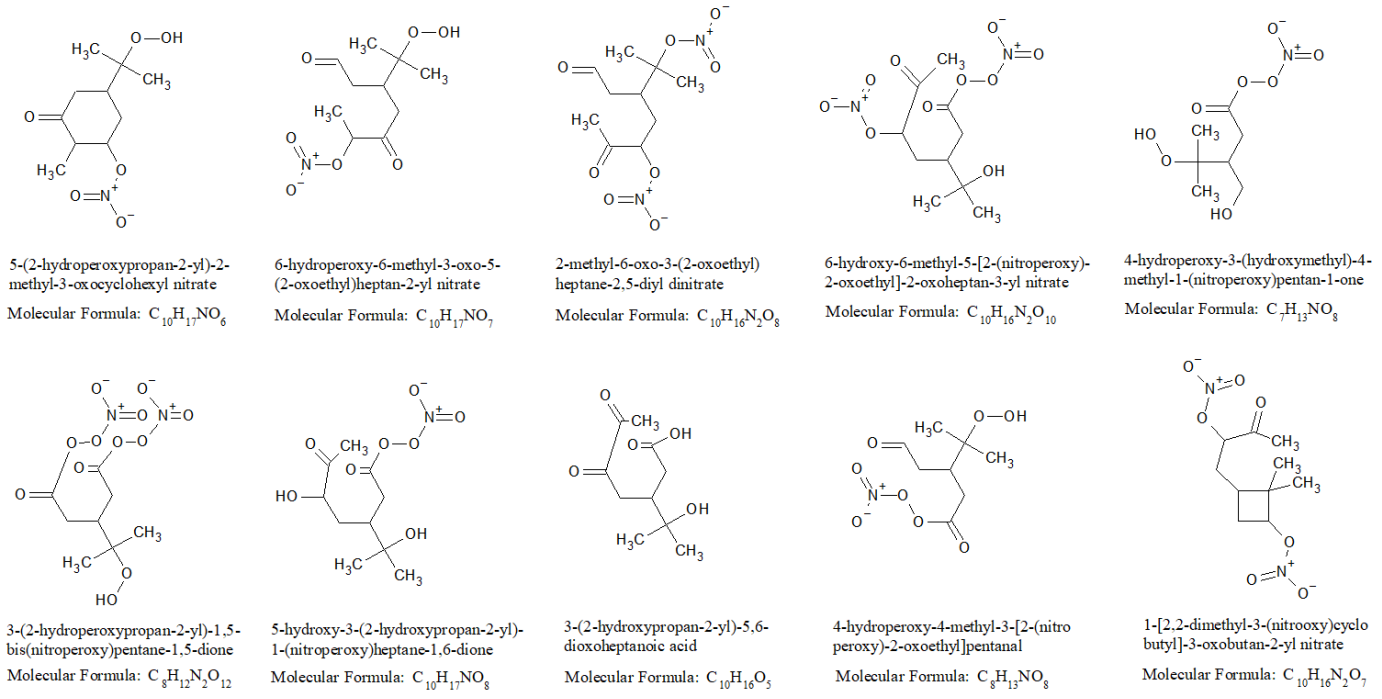

Figure S23: Top 10 particle-phase products from α-pinene photooxidation at the end of the high hydrocarbon (P_HHC) simulations.

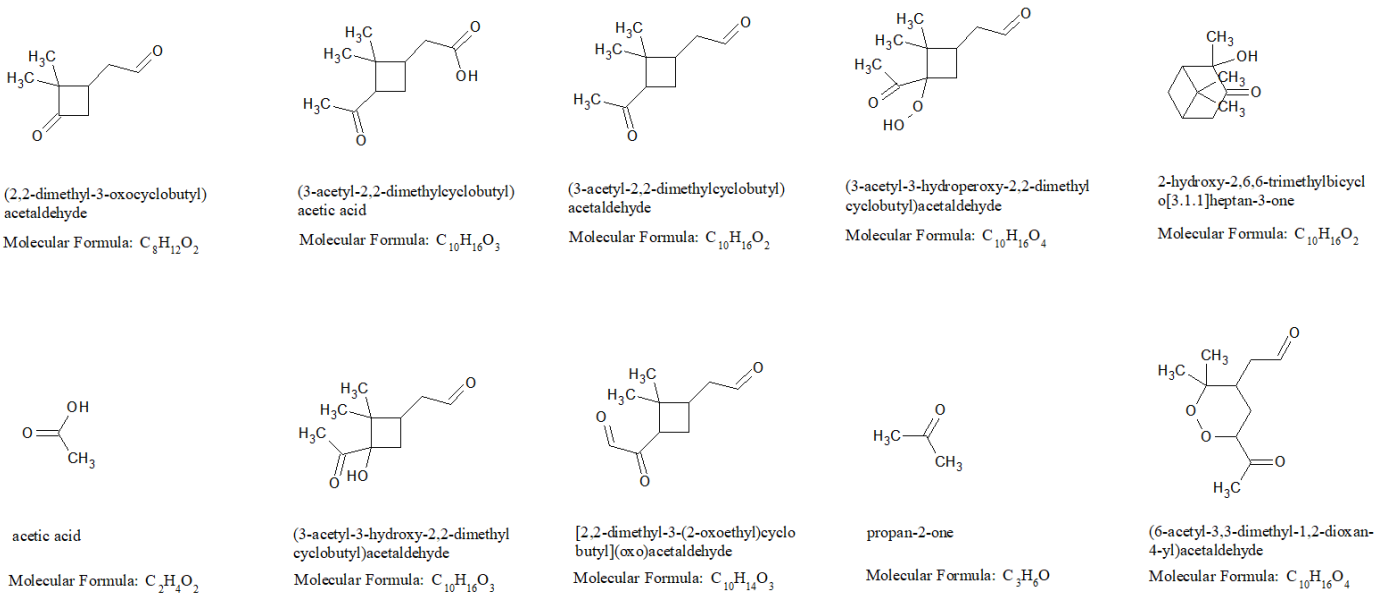

Figure S24: Top 10 gas-phase products from α-pinene dark ozonolysis at the end of the high hydrocarbon (DO_HHC) simulations.

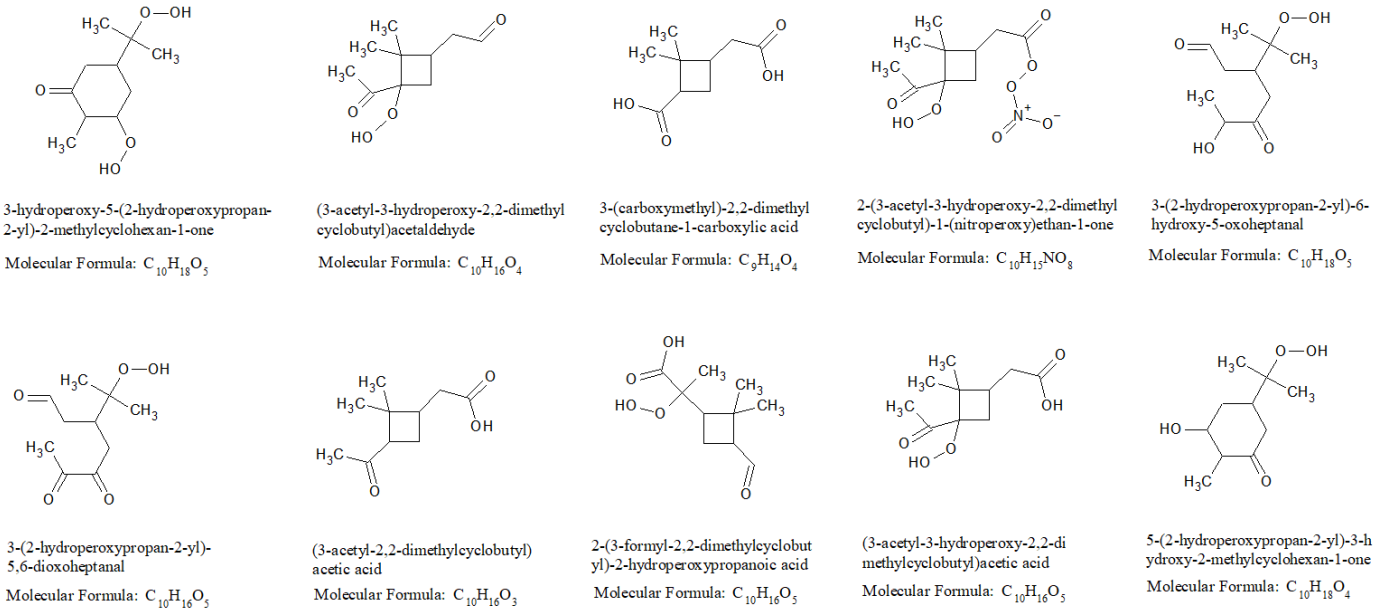

Figure S25: Top 10 particle-phase products from α-pinene dark ozonolysis at the end of the high hydrocarbon (DO_HHC) simulations.

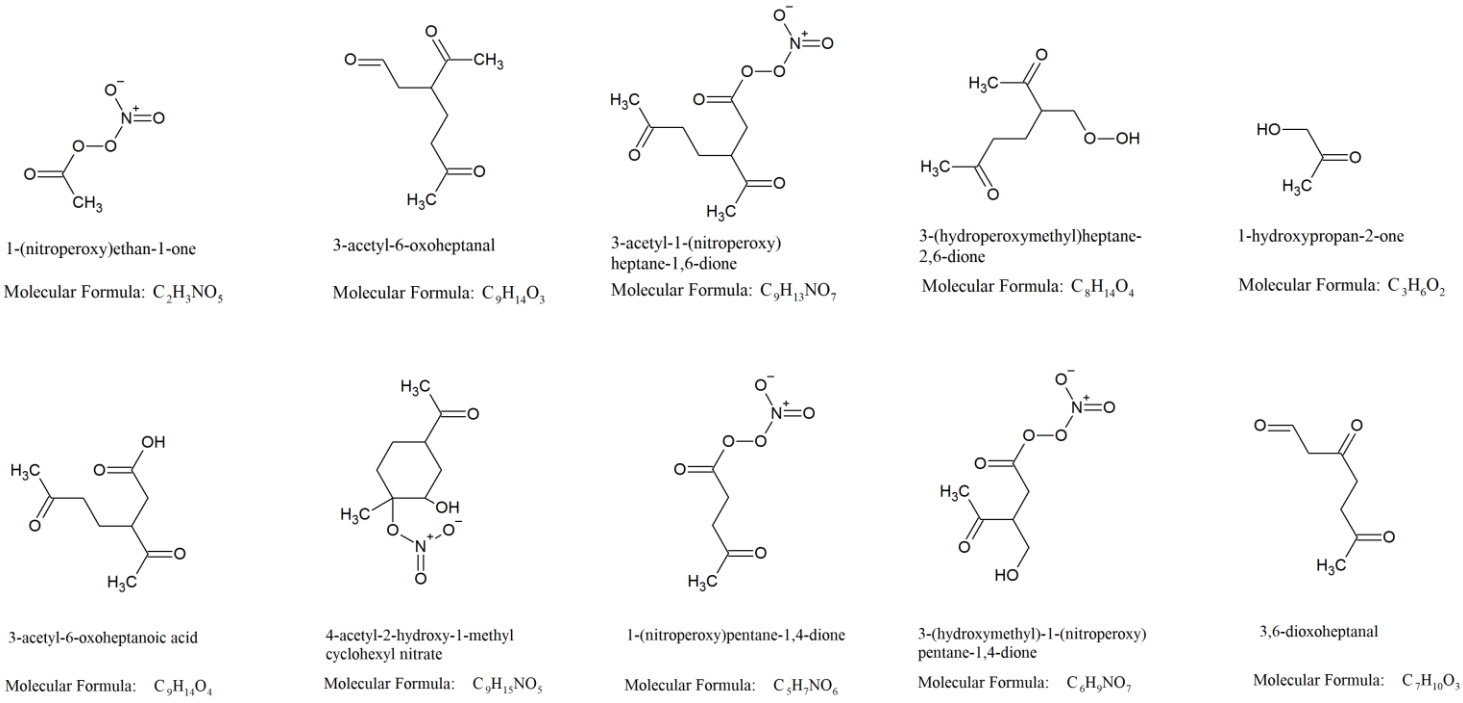

Figure S26: Top 10 gas-phase products from limonene photooxidation at the end of the high hydrocarbon (P_HHC).

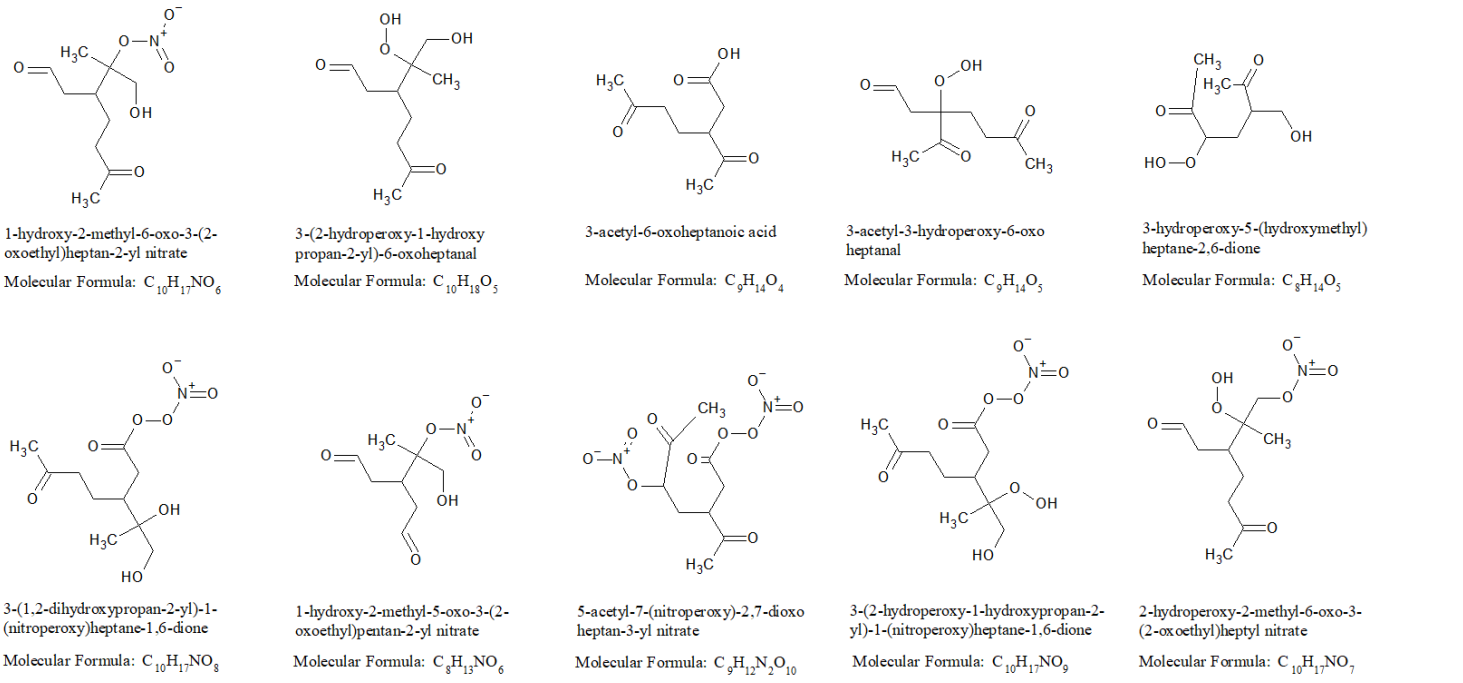

Figure S27: Top 10 particle-phase products from limonene photooxidation at the end of the high hydrocarbon (P_HHC).

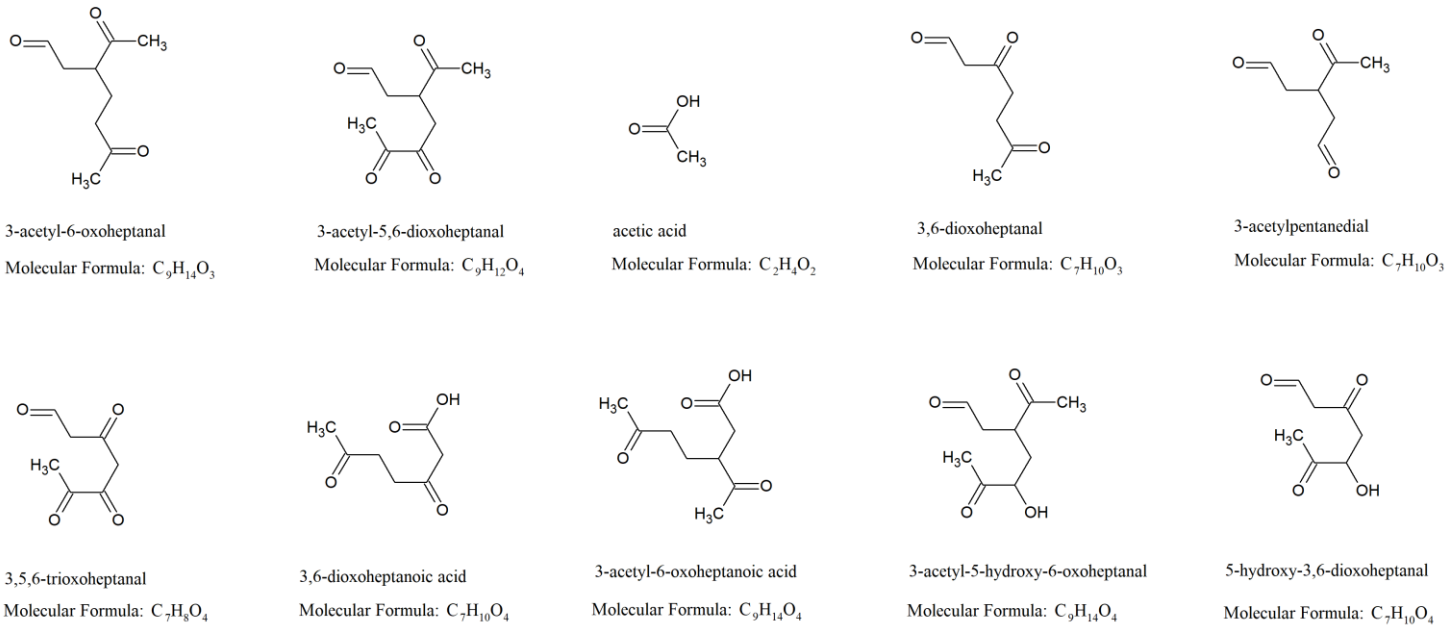

Figure S28: Top 10 gas-phase products from limonene dark ozonolysis at the end of the high hydrocarbon (DO_HHC).

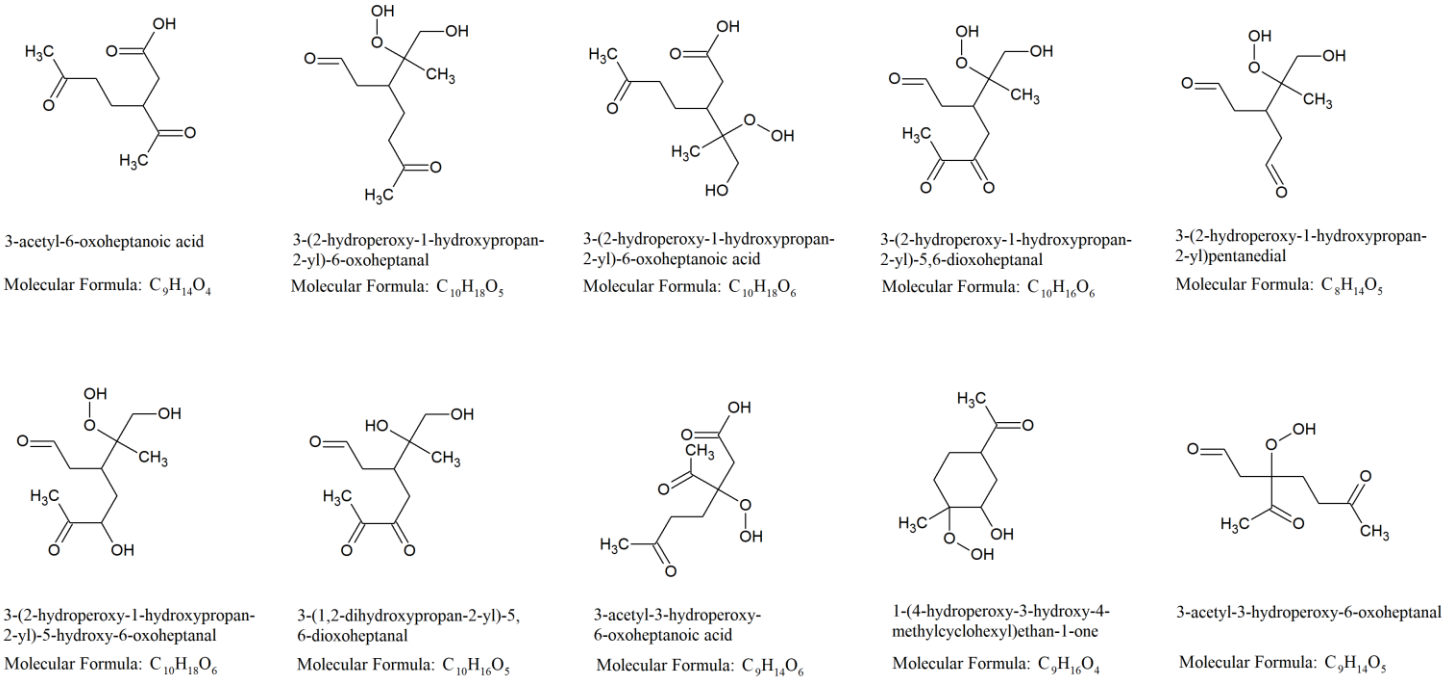

Figure S29: Top 10 particle-phase products from limonene dark ozonolysis at the end of the high hydrocarbon (DO_HHC).

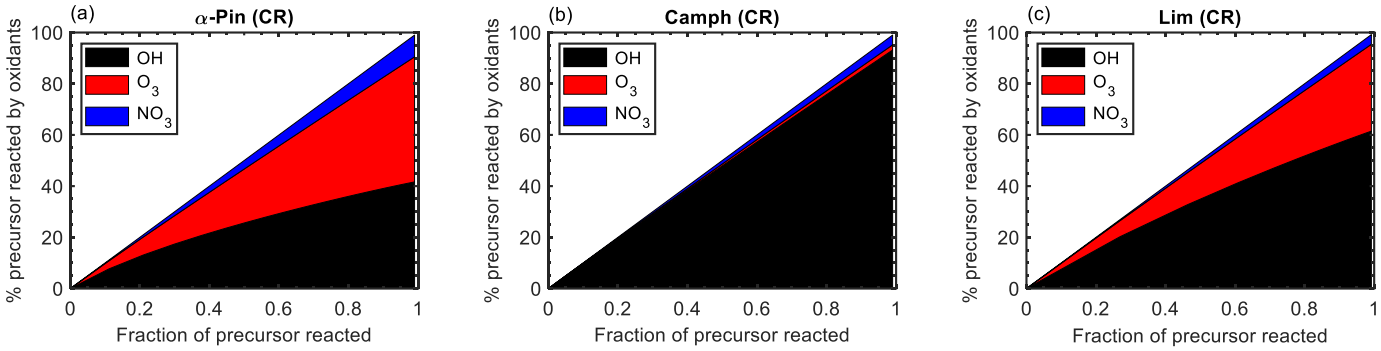

Figure S30: Percentage of precursor reacted by OH (black), O_3 (red), and NO_3 (blue) as a function of fraction of precursor reacted for α-pinene, camphene, and limonene during controlled reactivity (CR) simulations.

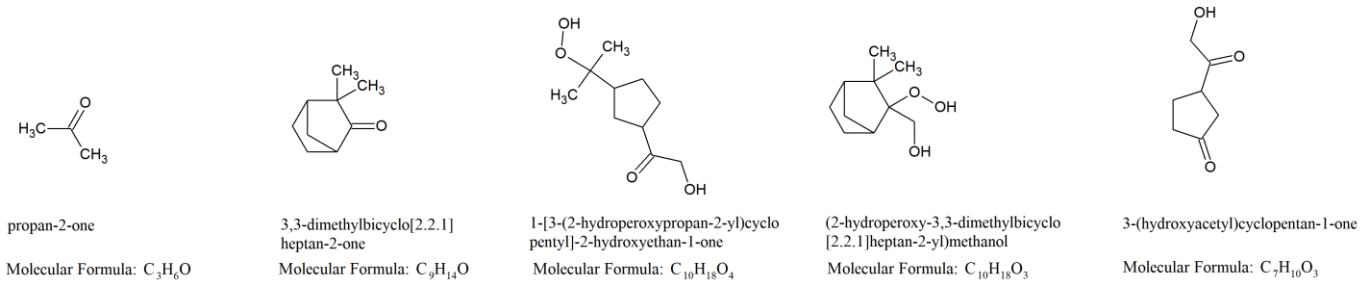

propan-2-one
Molecular Formula: C_3H_6O

3,3-dimethylbicyclo[2.2.1] heptan-2-one
Molecular Formula: $C_9H_{14}O$

1-[3-(2-hydroperoxypropan-2-yl)cyclo pentyl]-2-hydroxyethan-1-one
Molecular Formula: $C_{10}H_{18}O_4$

(2-hydroperoxy-3,3-dimethylbicyclo [2.2.1]heptan-2-yl)methanol
Molecular Formula: $C_{10}H_{18}O_3$

3-(hydroxyacetyl)cyclopentan-1-one
Molecular Formula: $C_7H_{10}O_3$

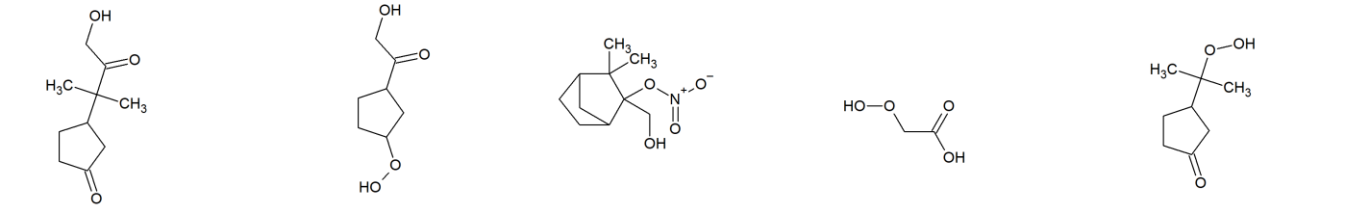

3-(4-hydroxy-2-methyl-3-oxo butan-2-yl)cyclopentan-1-one
Molecular Formula: $C_{10}H_{16}O_3$

1-(3-hydroperoxycyclopentyl)-2-hydroxyethan-1-one
Molecular Formula: $C_7H_{12}O_4$

2-(hydroxymethyl)-3,3-dimethylbi cyclo[2.2.1]heptan-2-yl nitrate
Molecular Formula: $C_{10}H_{17}NO_4$

hydroperoxyacetic acid
Molecular Formula: $C_2H_4O_4$

3-(2-hydroperoxypropan-2-yl) cyclopentan-1-one
Molecular Formula: $C_8H_{14}O_3$

Figure S31: Top 10 gas-phase products from camphene at the end of the controlled reactivity simulation.

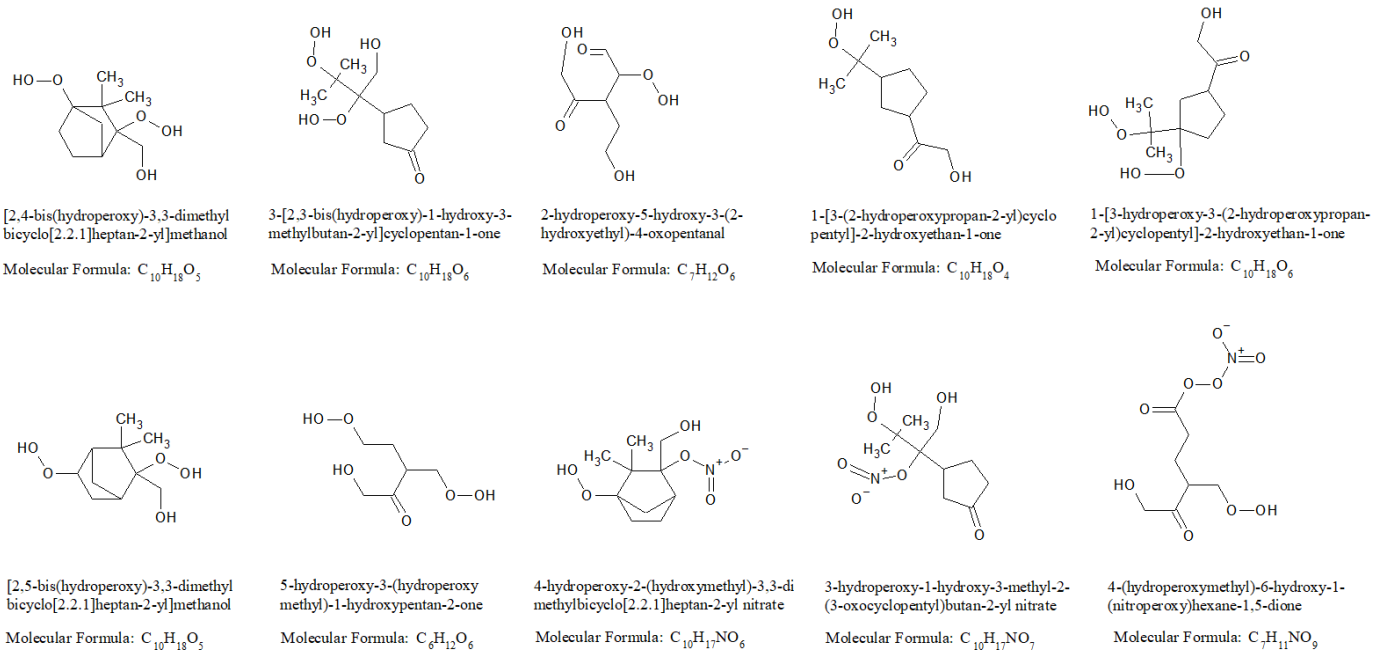

Figure S32: Top 10 particle-phase products from camphene at the end of the controlled reactivity simulation.

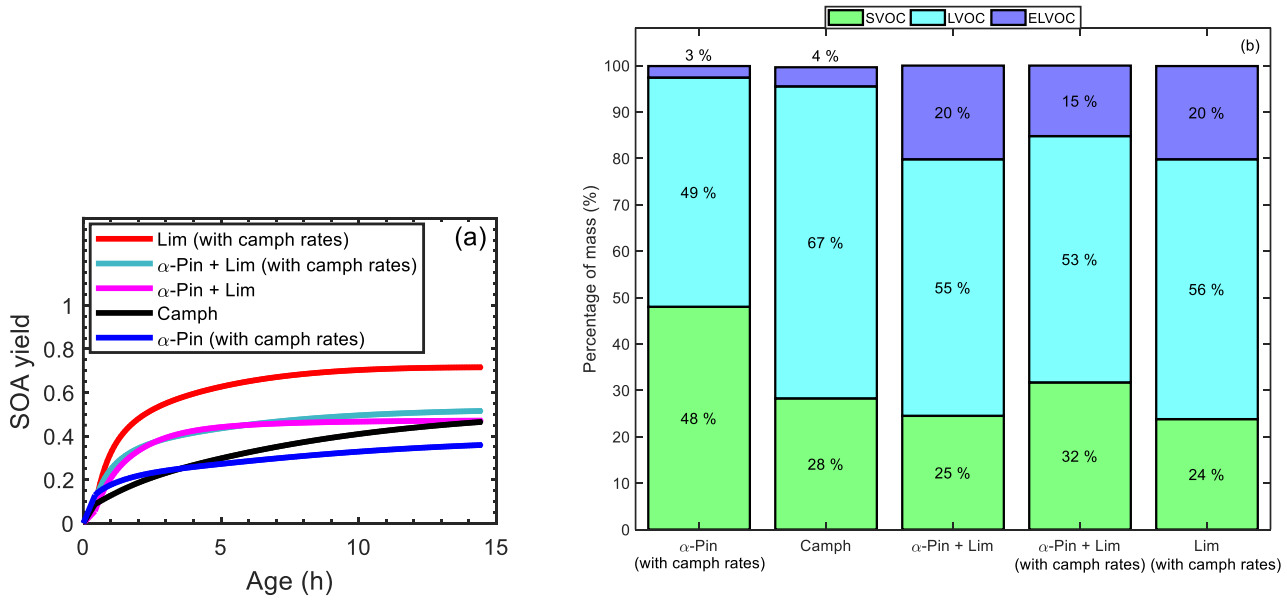

Figure S33: (a) Simulated SOA yield as a function of atmospheric aging time for: camphene (black line), 50 % α-pinene + 50 % limonene (magenta line), α-pinene with camphene rate constants (blue line), limonene with camphene rate constants (red line), and 50 % α-pinene + 50 % limonene where the rate constants of α-pinene and limonene were replaced with the rate constants of camphene (green line); and (b) mass percentage of particle-phase compounds binned in four volatility categories at the end of the controlled reactivity simulations for: camphene, 50 % α-pinene + 50 % limonene, α-pinene with camphene rate constants, limonene with camphene rate constants, and 50 % α-pinene + 50 % limonene where the rate constants of α-pinene and limonene were replaced with the rate constants of camphene.